Thermal design and performance evaluation of the BaR-SPOrt cryostat

M. Zannoni[a], C. Macculi[b], E. Carretti[b], S. Cortiglioni[b], G. Ventura[b], J. Monari[c], M. Poloni[c], S. Poppi[c]

[a]CNR I.A.S.F.-Milano, via Bassini, 15, I-20133 Milano Italy,
[b]CNR I.A.S.F.-Bologna, via Gobetti, 101, I-40129 Bologna Italy,
[c]CNR I.R.A.-Bologna, via Gobetti, 101, I-40129 Bologna Italy

ABSTRACT

To measure extremely faint signals like Cosmic Microwave Background Polarization (a few percent of CMB anisotropy) it is necessary to use very high sensitivity radiometers. This means to adopt low noise cryogenic front-end and long integration times. This is the case of BaR-SPOrt (Balloon borne Radiometer for Sky Polarization Observations), an experiment designed to measure the CMB polarization at sub-degree angular scales. In the millimeter range, where coherent radiometers (polarimeters) are typically employed, usual mechanical coolers can represent a limit to the final sensitivity due to their base temperature instability. As a matter of fact, in correlation polarimeter, temperature fluctuations of the front-end devices, can both mimic a polarized signal and severely limit instrumental sensitivity. Here we discuss in detail the thermal design of the cryostat housing the instrument with particular attention to the closed loop cryocooler adopted, which is able to guarantee 6W at 77K with a stability better than 0.1 K over several hours.

Keywords: Cosmology, CMB, Polarimetry, Cryogenics, Instrumentation, LDB

1. INTRODUCTION

BaR-SPOrt experiment[1] is aimed at measuring Cosmic Microwave Background Polarization (CMBP) at sub-degree angular scales. The extremely low signal to be measured, at the level of μK, asks for extremely high sensitivity polarimeters and long integration time in very stable environmental conditions. As a matter of fact, the key point for long integration time experiments is the signal stability, being the long term gain fluctuation ($\frac{\Delta G}{G}$) and offset instability the main sources of sensitivity degradation. Both these effects are driven and/or boosted by temperature fluctuations, so accurate thermostability is crucial. Taking into account these effects, the radiometer sensitivity equation can be generalized as follows[2]:

$$\Delta T_{rms} = \sqrt{\frac{k^2 T_{sys}^2}{\tau \Delta\nu} + T_{offset}^2 \Big(\frac{\Delta G}{G}\Big)^2 + \Delta T_{offset}^2} \tag{1}$$

where the first term is the usual radiometer formula where τ and $\Delta\nu$ are the integration time and bandwidth respectively, T_{sys} the system noise temperature and k a parameter related to the radiometer type. The second and third terms take into account the gain fluctuations which modulate the offset equivalent temperature and the offset fluctuations themselves. From equation 1, to maximize the sensitivity it is necessary to reduce T_{sys}, i.e. to employ low noise cryogenic front ends, minimize T_{offset} and both gain and T_{offset} fluctuations. To meet these two requirements the common solution is to operate the radiometer at the lowest achievable temperature and to employ appropriate data reduction techniques (like destriping[3]). Since the only cooling might not be able to minimize the off-set impact, in BaR-SPOrt we have operated towards two directions: the first one was to improve the performances of the devices where T_{offset} is generated,[4,5] the Polarizer and Ortho-Mode Tranducer, and the second one was to cool these devices at 80K with a mechanical cryocooler able to keep the base temperature as

Further author information: (Send correspondence to M. Zannoni)
M. Zannoni: E-mail: zannoni@mi.iasf.cnr.it
Address: Istituto di Astrofisica Spaziale e Fisica Cosmica sezione di Milano, via Bassini 15, I-20133 Milano Italy

stable as ±0.1K. The temperature equivalent off-set generated by the antenna system of a correlation polarimeter like the BaR-SPOrt one is given by[4]

$$T_{offset} = SP_{OMT}(T_{sky} + T_{Noise}^{Ant}) + SP_{pol}\left(T_{sky} + T_{Noise}^{Horn} - \frac{T_{ph}^{Pol}}{\eta}\right) \quad (2)$$

where T_{sky} is the signal coming from the sky, T_{Noise}^{Horn} is the noise generated by the feed horn alone, T_{Noise}^{Ant} the one of the whole antenna system, η is the horn transmission coefficient and T_{ph}^{Pol} is the physical temperature of the polarizer. SP_{OMT} and SP_{POL} are two coefficients related to the off-set generation performances of the two devices: SP_{OMT} takes into account for the cross-talk between the two arms of the OrthoMode Transducer, while SP_{POL} measures the difference of the transmission coefficients of the two polarization states of radiation propagating in the Polarizer. Our collaboration has settled new state of the art polarizer and OMT performances[5] and now T_{offset} is as low as $\sim$ 50 mK.* From equation 2 it is also clear that the stability of the physical temperature of the antenna system (horn, polarizer and OMT) is crucial.[6] For this reason in the whole radiometer the different working temperatures are stabilized better than ±0.1 K. In this paper we focus on the BaR-SPOrt cryostat where all the receiver is housed. In fact the high vacuum necessary to the thermal isolation of the cryogenic components can be exploited to create the appropriate environmental isolation for all the critical parts of the polarimeter, definitely improving all the thermal stability of the receiver.

2. THE CRYOSTAT

The BaR-SPOrt cryostat is an AISI-304 stainless-steel chamber designed to house both the warm ($\simeq$ 300 K) and the cold ($\simeq$ 80 K) parts of the polarimeter (Fig. 1). On the base of the chamber there are the electrical feed-throughs and the main pumping line where a turbo-molecular pump is attached. During the balloon flight, where the turbo pump can fail, the vacuum is maintained by both the cold part of the radiometer which, being at 80 K, has a moderate pumping efficiency and a couple of getter pumps by Saes Getters®. The electrical connections are based on four Ceramaseal® 41 pins MIL-C-26482 type connectors. They serve both the thermostats of the warm sectors and all the electronics inside, including in/out data transfer. Both cold and warm devices are housed inside

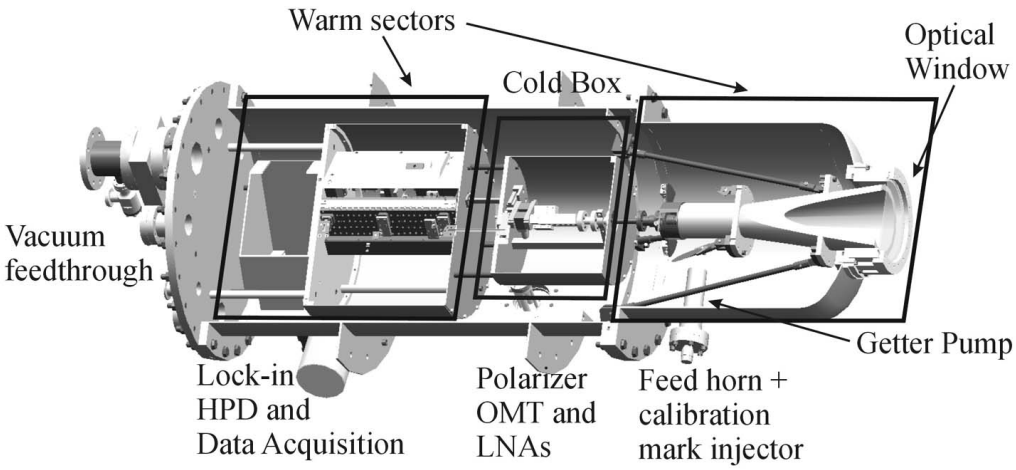

Figure 1. BaR-SPOrt vacuum chamber.

the cryostat. This choice is driven by two necessities: the first one is to keep the two arms of the polarimeter (for

*Another offset source, in systems like BaR-SPOrt, is the vacuum window. A detailed study of the spurious polarization (see Macculi et al., this volume) produced by such a dielectric shows that by choosing a teflon window the maximum effect introduced in our band [30.4 - 33.6 GHz] is $\tilde{0}$.14 mK, negligible with respect to the antenna offset.

a detailed description of the radiometer architecture see Ref.[7] and Ref.[1]) balanced for what about gain and phase and this is easier if all the receiver is inside the vacuum chamber, avoiding RF vacuum windows. The second reason is that any radio-astronomy receiver is extremely sensitive to its physical temperature variations so the high vacuum necessary to the cryogenic front-end is employed to isolate and thermally stabilize the warm part of the instrument too. Due to the limited cooling capability of the cooler, an accurate thermal budget has been studied. This budget takes into account for radiative and conductive heat load on the cooler, the latter coming from the waveguides (mainly) which are thin wall stainless steel, with the circular one connecting the calibrator (warm) and the polarizer (cold) being $5\mu m$ silver coated to minimize its insertion loss and from the phosphor bronze wires for LNAs bias and thermometers (PT100). The heat dissipated by the LNAs has been taken into account too, their electrical power consumption being adopted as an upper limit. The radiative heat charge can be efficiently shielded by means of aluminized mylar (superinsulation) thanks to the simple geometry of the cryostat. In figure 2 the thermal budget of the heat entering the cold box versus the number of superinsulating sheets is presented. From the simulation we have estimated a heat charge lower than 1.5 W at 80 K. The budget

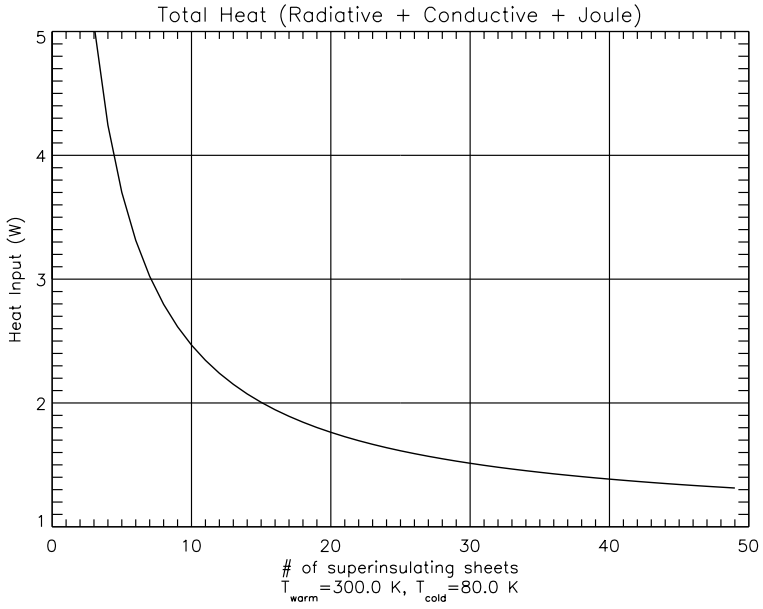

Figure 2. BaR-SPOrt thermal budget.

breakdown is presented in Table 1. As described in the next section, this evaluation must be compared with the characteristics of the cooling method employed, liquid cryogens or mechanical coolers.

$\dot{Q}_{cond}$	0.30 W (silver coat. circ. waveg.) 0.35 W (2 rectangular waveguide) 0.05 W (phosphor bronze wires) 0.26 W (fiberglass holders)
$\dot{Q}_{rad}$	0.33 W (50 superins. sheets)
$\dot{Q}_{joule}$	0.04 W (LNAs)
$\dot{Q}_{TOT}$	1.33 W

Table 1. Thermal budget breakdown.

3. THE COOLER

As described in Ref,[8] due to the simple optical scheme necessary to minimize spurious polarization, we adopted an on-axis cassegrain configuration to achieve sub-degree angular resolution. The main consequence is that the receiver moves together with the telescope. This fact seriously limits the possibility to adopt a liquid cryogen to cool the receiver front-end because the telescope must move from the zenith "parking" position in the ascending phase to the almost horizontal one when observing the sky. Moreover, the need for long holding time (a LDB flight can be definitely longer than 15 days) with the consequent large storage volume for cryogens, moved our choice to cryocoolers. However standard mechanical cooler are generally not compatible with balloon flights: designed to have high cooling powers, they are heavy, electrical power thirsty, with low efficiency. Moreover laboratory cryocooler are typically open loop, which means that the base temperature depends both on the heat charge on the cold stage and on the effective heat dissipation of the compressor, with the consequence that the cold finger temperature may be not as stable as required by CMBP experiments. In BaR-SPOrt we have adopted a compact, lightweight, low electrical power demanding, closed loop cryocooler model POLAR SC-7 COM made by Leybold-Vacuum GMBH (see figure 3). The cooler is based on single stage Styrling cycle. Nominal cooling

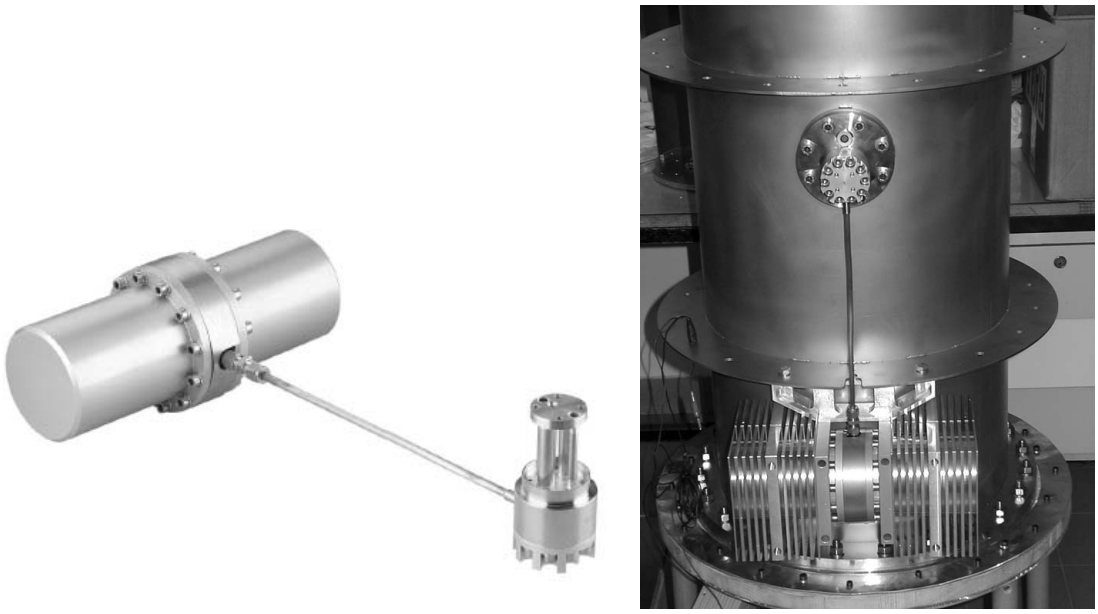

Figure 3. Cryo-cooler Leybold Polar SC-7. On the left there is the cooler alone, on the right it is visible mounted on the BaR-SPOrt cryostat with the compressor heat dissipators.

power is 6W @ 77 K with an electrical power drain of 250W. This model is PID controlled, resulting in a nominal temperature stability of ± 0.1 K. Tests have been performed to verify:

1. the cooling power
2. the cold finger temperature stability

Concerning the first test, heat has been injected by an heater directly linked to the cold finger while the compressor power drain (PIN) has been measured. During the second test, no heat has been applied to the cold finger and its temperature has been monitored for about 6 days.

3.1. Test 1: cooling capability

The test has been performed by setting the cold finger temperature at 60 K to probe the cooler near the limit of the working region but still where the temperature stability can be achieved (nominally 35 K is the minimum

temperature attainable with zero heat charge, but in this condition the power drain is the maximum allowable, 250 W, and the temperature control is not efficient). In Fig. (4) the plot of the experimental data is shown. The

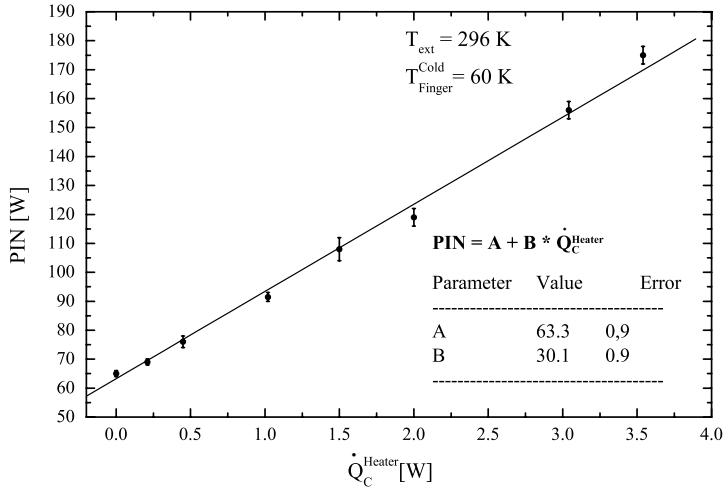

Figure 4. Stand alone test experimental data. A linear fit is also shown. $T_{\rm ext}$ is the cryostat external temperature. The error bars associated to each point represent the amplitude of the fluctuations of the compressor power drain necessary to guarantee the temperature set point.

total thermal input absorbed by the cold finger is the sum of the heat dissipated by the heater plus the parasitic inputs (conductive heat from the heater wires, residual radiative heat and so on). Thus, the curve plotted in Fig. (4) represents a lower limit of the cold finger cooling capability. Such a test shows that the cooler works very well, with low power consumption. The 1.5 W @ 80K estimated for BaR-SPOrt corresponds, according to our experimental data @ 60 K, to an upper limit of 110 W of electrical power drain.

3.2. Test 2: cold finger temperature stability

The test has been performed at $T_{CF} = 80$ K. The temperature has been measured by means of a calibrated Rhodium-Iron sensor and acquired every 30 s by means of a digital ohmmeter. Such data have been analyzed in time and frequency domains in order to know the stability around the mean value and the stability time scale by the density power spectrum of the cold finger temperature. Data have been acquired for about 6 days and are plotted in Fig. (5).
The plot shows that the stability of the cold finger temperature, $\sigma_{T_{CF}}$, is well below 0.1 K which is the thermal specification of the experiment. In particular, the peak-to-peak amplitude (T_{CF}^{PP}) is lower than 0.1 K.

The last parameter to be tested is the long term-stability, which can be obtained by the power spectrum of the cold finger temperature: see Fig. (6).
The power spectrum is featured by: $1/f$ plus white noise plus three spikes plus low-pass spectra. Since the sampling interval is 30 s then the spectrum is cut at the Nyquist frequency $f_{\rm Ny} \sim 0.017$ Hz. The low pass filtering is due to the integrator of the digital voltmeter. Probably also the three spikes are an effect introduced by the ohmmeter. In order to have an idea of the cold finger temperature stability we performed a fit on its spectrum defined as:

$$S_{T_{\rm CF}}(f) = \sigma_0^2 \left[1 + \left(\frac{f_k}{f} \right)^{\beta} \right] \tag{3}$$

In Fig. (6) and in Table (2) the fit and its parameters are shown.

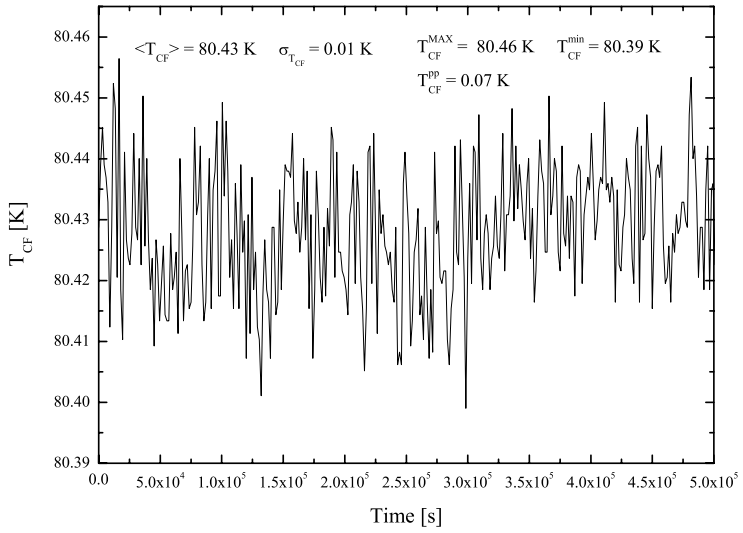

Figure 5. Cold finger temperature data stream. T_{CF} is the cold finger temperature. See text for details.

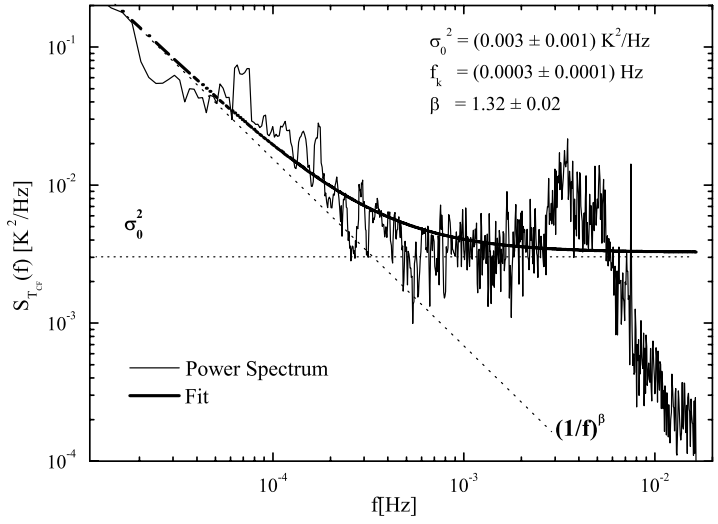

Figure 6. Fit on the cold finger temperature power spectrum. See text for details.

Before the integrator cut-off the spectrum is characterized by a low frequency noise with a knee at $f_k = 0.34$ mHz. That is the thermal stability (white noise plateau) is guaranteed up to $t_k = 1/f_k \simeq 3000\ s$, which is a time greater than the scanning period of the telescope ($\sim$ minutes).
This is an important result. If the origin of the offset fluctuations generated by the devices enclosed in the cold box is their temperature instability, they are expected to be "stable" during the telescope scanning period.

σ_0^2 [K^2/Hz]	f_k [Hz]	β
0.003 ± 0.001	0.0003 ± 0.0001	1.32 ± 0.02

Table 2. Fitting function parameters. σ_0^2 identifies the white noise plateau, f_k and β are the knee frequency and the spectral index of the $1/f$-like noise, respectively.

Performances get definitely better when all the devices to be cooled are connected to the cold finger, greatly increasing the heat capacity of the system. Some results are reported in section 4.

4. PRELIMINARY TESTS

In this section we present the preliminary tests of the cryostat performances with the radiometer assembled inside in an almost final configuration. The only difference, for what about the cold box, is that the LNAs have been replaced with dummies, since the thermal budget isn't dominated by their dissipation. During this run, the temperature of the warm part of the radiometer was regulated by an OMRON® thermoregulator. The power supplied requested by the cooler compressor was PIN = 93 W, and the temperature cold finger set was 75 K. In order to have a good thermoregulation, the temperature set point of the parts managed by the OMRON, must be higher than the chamber temperature. Thus, we regulated the warm part temperature at $\sim$ 308 K.
In order to have an idea of the thermoregulation efficiency, in Fig. (7) we compare the temperature trend of the warm part of the radiometer (marked as S-guide on the plot) when the OMRON is switched on and off. The S-guides are two waveguides connected to the warm end of the rectangular thermal chokes attached to the output of the cooled HEMT amplifiers. Hence, the S-guide can be considered as a good tracer of the warm part of the radiometer. As shown in figure 7, the OMRON is able to provide a very good temperature stability (0.2

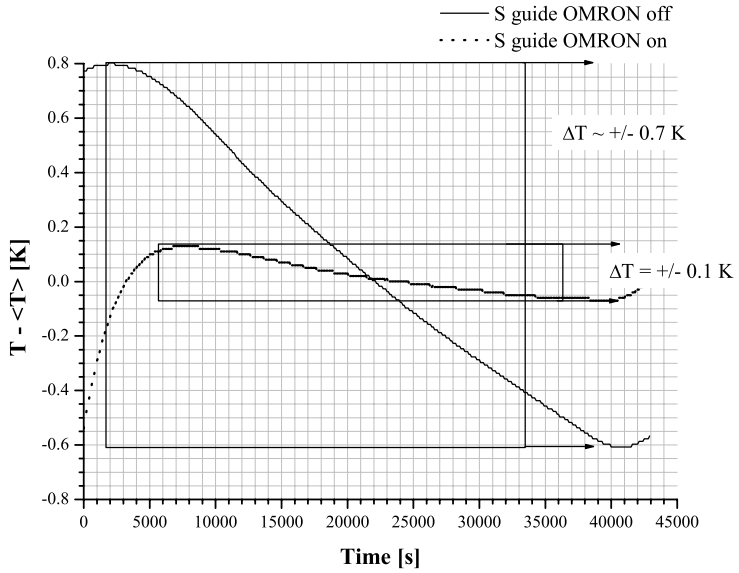

Figure 7. Comparison of the S-guide temperatures during OMRON on and off configuration. The residuals with respect to their mean values are plotted. The corresponding peak-to-peak variation of chamber temperature was ± 0.9 K.

K peak-to-peak) for the warm parts. Finally, in Fig. (8) the temperature stability of the cold section is shown. Over a time scale of 10^4 s, the temperature stability is around 0.05 K. By considering the typical scanning period

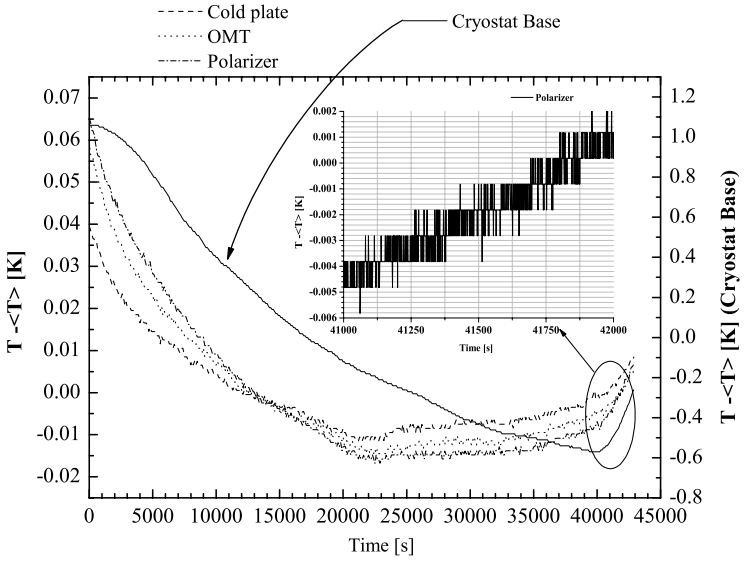

Figure 8. Temperature Stability of the cold section compared with the chamber temperature. A detail of the polarizer temperature is also shown.

of the BaR-SPOrt telescope (some minutes), the figure shows that the stability of the polarizer temperature over 300 s is 0.002 K peak-to-peak. Such fluctuation data have been extracted during a period of fast temperature variation as shown in the zoomed plot. Thus the 0.001 K fluctuation can be considered as worst case.

5. CONCLUSIONS

The preliminary tests of the BaR-SPOrt cryostat and cooling system show a very good thermal design of the instrument. This translates in an outstanding performance of the cryocooler in term of temperature stability and power consumption, confirming this device as a real alternative to liquid cryogens for long duration balloon flights. The very high stability of the temperature of both the warm and cold parts of the radiometer let us conclude that thermal instabilities represent a source of offset fluctuation negligible for BaR-SPOrt.

ACKNOWLEDGMENTS

Authors wish to thank A.S.I. (Italian Space Agency) for the full support to BaR-SPOrt and P.N.R.A. (National Project for Research in Antarctica) for its relevant contribution. MZ, CM and SP thank ASI for their grant in the frame of the SPOrt program.

REFERENCES

1. M. Zannoni, S. Cortiglioni, G. Bernardi, E. Carretti, S. Cecchini, C. Macculi, E. Morelli, C. Sbarra, G. Ventura, L. Nicastro, J. Monari, M. Poloni, S. Poppi, V. Natale, M. Baralis, O. Peverini, R. Tascone, G. Virone, A. Boscaleri, E. Pascale, G. Boella, S. Bonometto, M. Gervasi, G. Sironi, M. Tucci, R. Nesti, R. Fabbri, P. De Bernardis, M. DePetris, S. Masi, M. V. Sazhin, and E. N. Vinyajkin, "The BaR-SPOrt experiment," in *Polarimetry in Astronomy. Edited by Silvano Fineschi . Proceedings of the SPIE, Volume 4843, pp. 324-335 (2003).*, pp. 324–335, Feb. 2003.
2. E. J. Wollack, "High-electron-mobility-transistor gain stability and its design implications for wide band millimeter wave receivers," *Review of Scientific Instruments* **66**, pp. 4305–4312, Aug. 1995.

3. C. Sbarra, E. Carretti, S. Cortiglioni, M. Zannoni, R. Fabbri, C. Macculi, and M. Tucci, "An iterative destriping technique for diffuse background polarization data," *Astronomy and Astrophysics* **401**, pp. 1215–1222, Apr. 2003.
4. E. Carretti, R. Tascone, S. Cortiglioni, J. Monari, and M. Orsini, "Limits due to instrumental polarisation in CMB experiments at microwave wavelengths," *New Astronomy* **6**, pp. 173–187, May 2001.
5. E. Carretti, S. Cortiglioni, C. Macculi, C. Sbarra, G. Ventura, J. Monari, M. Poloni, S. Poppi, V. Natale, R. Nesti, M. Baralis, O. Peverini, R. Tascone, G. Virone, G. Sironi, and M. Zannoni, "High Stability and Sensitivity Correlation POlarimeters for CMB Polarization Measurements," in *This Proceeding*,
6. E. Carretti, M. Zannoni, C. Macculi, S. Cortiglioni, and C. Sbarra, "Effects of Thermal Fluctuations in the SPOrt Experiment," *Astronomy and Astrophysics Submitted* .
7. S. Cortiglioni, G. Bernardi, E. Carretti, L. Casarini, S. Cecchini, C. Macculi, M. Ramponi, C. Sbarra, J. Monari, A. Orfei, M. Poloni, S. Poppi, G. Boella, S. Bonometto, L. Colombo, M. Gervasi, G. Sironi, M. Zannoni, M. Baralis, O. A. Peverini, R. Tascone, G. Virone, R. Fabbri, V. Natale, L. Nicastro, K.-W. Ng, E. N. Vinyajkin, V. A. Razin, M. V. Sazhin, I. A. Strukov, and B. Negri, "The Sky Polarization Observatory," *New Astronomy* **9**, pp. 297–327, May 2004.
8. E. Carretti and et al., "SPOrt: an Experiment Aimed at Measuring the Large Scale Cosmic Microwave Background Polarization," *this volume* .